Eur Biophys J (1997) 25: 481–487

ARTICLE

Harvey K. Shepard · Timothy J. Wilson
Thomas P. Moody · John O. Wooll · Thomas M. Laue

Determination of macroion diffusion coefficients using an analytical electrophoresis apparatus

Accepted: 4 October 1996

Abstract Methods are presented to determine the effective macroion diffusion coefficient in the presence or absence of an electric field, using a unique analytical electrophoresis apparatus in which both electrophoretic mobility and steady-state electrophoresis may be studied. Approximate analytic solutions to the differential equations and boundary conditions describing diffusion are derived. These solutions are shown to be good approximations to numerial simulations of the differential equations, and provide a good phenomenological description of experimental data for the oligonucleotide $p(dA)_{20} \cdot p(dT)_{20}$ in 100 mM KCl, 20 mM Tris-HCl, pH 8.0 buffer. Diffusion and electrophoresis measurements are made on a single sample without changing the buffer or the macroion concentration, thus the data are directly comparable.

Key words Analytical electrophoresis · Diffusion · Macromolecules · Simulations

Introduction

Charge is a fundamental property of macromolecules that is inextricably linked to their structure, solubility, stability and interactions. The most direct means of discerning a macroion's effective charge in solution is by its response to an applied electric field. However, a macroion's behavior is complicated by its connection with the behavior of the surrounding mobile ionic atmosphere (Henry 1931; Onsager 1932; Booth 1950; Overbeek and Wiersema 1967). A unique analytical electrophoresis apparatus (AEA) developed in our laboratory permits both the measurement of macroion electrophoretic mobilities and the determination of steady-state electrophoresis concentration distributions (Laue et al. 1989; Ridgeway et al. 1994; Laue et al. 1996). Interpretation of this electrophoretic data requires knowledge of the frictional and diffusion coefficients of the macroion. In this paper we present methods for the determination of macroion diffusion coefficients both in the presence and absence of an electric field using the AEA. Diffusion and electrophoresis measurements may be made on a single sample without changing the arrangement of the apparatus.

T. J. Wilson · T. P. Moody · J. O. Wooll · T. M. Laue (✉)
Department of Biochemistry and Molecular Biology, Rudman Hall, University of New Hampshire, Durham, NH 03824-3544, USA

H. K. Shepard
Department of Physics, University of New Hampshire, Durham, NH 03824-3544, USA (e-mail: shepard@curie.unh.edu)

Experimental

Instrument. A detailed description of the AEA has been presented elsewhere (Ridgeway et al. 1994). Briefly, the instrument is an imaging spectrophotometer using a linear photodiode array to measure the light intensities from up to 512 positions along a fused-silica cuvette. The cuvette's cross-section is 2×2 mm, and its top and bottom are open. Cuvettes with distances of 2 mm and 4 mm between the openings are available. The open ends of the cuvette are sealed by semi-permeable membranes, which permits the establishment of an electric field along the cuvette's length while retaining macroions in the field of view.

Materials. All buffers and salts were reagent grade and were used without additional purification. Equimolar mixtures of single stranded $p(dA)_{20}$, Pharmacia #27-7984-01, and $p(dT)_{20}$, Pharmacia #27-7841-01, were heated to 65 °C in 200 mM KCl, 20 mM Tris-HCl, pH 8.0 buffer, then cooled to form double stranded $p(dA)_{20} \cdot p(dT)_{20}$. Melting and circular dichroism studies were used to verify that $p(dA)_{20} \cdot p(dT)_{20}$ was in a stable duplex form under the conditions of electrophoresis, and capillary zonal electrophoresis was used to test for sample homogeneity (not shown). Concentrations were estimated from the A_{260} measured in the apparatus.

Experimental procedures. Steady-state electrophoresis and mobility experiments were performed at 20±0.1 °C as described previously (Laue et al. 1996). Diffusion in the absence of an electric field was observed by first establishing a steady-state macroion gradient, and then recording the collapse of the gradient at regular time intervals after the exernal field was turned off. Current was supplied by a Keithley 224 programmable current source and field strengths were calculated using specific conductivities measured with an VWR Scientific 1054 conductivity meter. The specific conductivity is not affected measurably by DNA oligonucleotides at the concentrations used here. Experiments using voltage sensing electrodes have verified the accuracy of the calculated fields (not shown). The buffer flow was adjusted until the pH of the effluents from the cathode and anode electrode chambers were within 0.1 unit of the initial pH.

Computer simulations. The simulation uses a finite-difference approach such as that previously applied to sedimentation (Cox 1965; Cox and Dale 1981). Here, however, a rectangular cell replaces a sector shaped cell and the simulation involves an electric field acting on a charge rather than a gravitational field acting on a mass. The cell is divided along its length into a set of volume elements, each of length Δx. Macroions move between neighboring volume elements during a set time interval (t_i). The properties of the system are used to calculate the amount of material moved between volume elements in each time interval. The properties used in these calculations include the concentration of macroions in each volume element prior to a given time interval, the electric field strength, the macroion diffusion coefficient, the temperature (set to 293.15 K), and the effective charge of the macroion (set to 8.6 proton equivalents). ANSI C or Windows versions of the program are available at http://www.bbri.harvard.edu.

Theory and results

In this work we shall not consider all of the complications of coupled diffusion (Onsager, 1945; Gosting, 1956), in which the flows of each charged species are linked due to the forces between the macroion and the salt ions comprising the ionic atmosphere and the requirement of local charge and current conservation. Instead, we assume that macroion motion can usefully be described by a simpler theory, with the coupled flow effects being summarized in effective phenomenological macroion diffusion and frictional coefficients. We also are implicitly assuming that our irreversible thermodynamic system is *near* equilibrium at all times, so that the fluxes can be expanded (in a linear approximation) about their equilibrium values.

Assuming one-dimensional motion, diffusion causes a flow of macroion

$$J_D = - D \, \partial c/\partial x \, , \tag{1}$$

where $c(x, t)$ is the macroion concentration and D the phenomenological diffusion coefficient. The force due to the external electric field, E, in the x-direction produces a flux of macroions

$$J_E = c \, v = c \, \mu \, E \, , \tag{2}$$

where v is the constant velocity acquired due to the balance of forces, and μ is the mobility ($\mu \equiv v/E$) of the macroions, assumed to be independent of the concentration. (We are ignoring the fact that the effective electric field acting at the macroion may not be the same as the external field.)

Thus, the total current, due to both diffusion and the external field, will be

$$J = - D \, \partial c/\partial x + c \, \mu \, E \, . \tag{3}$$

The continuity equation (conservation of macroions), $\partial c/\partial t = \partial J/\partial x$, implies

$$\partial c/\partial t = D \, \partial^2 c/\partial x^2 - \mu \, E \, \partial c/\partial x \, , \tag{4}$$

where we assume that D is independent of concentration (in the range of our experiments) and hence independent of x. The boundary condition is that no macroions can pass through the membranes:

$$J = 0 \;\; \text{at} \;\; x = 0 \;\; \text{and} \;\; x = L \, , \tag{5}$$

where J is given by Eq. (3).

Determining D when E = 0: To determine the zero field diffusion coefficient we use a slight variant of the method of Harned and French (1945). With E = 0, J reduces to J_D, and Eq. (4) reduces to the simple diffusion equation

$$\partial c/\partial t = D \, \partial^2 c/\partial x^2, \tag{6}$$

with the boundary condition

$$\partial c/\partial x = 0 \;\; \text{at} \;\; x = 0 \;\; \text{and} \;\; x = L \, . \tag{7}$$

Standard separation of variables applied to Eqs. (6) and (7) leads to

$$c(x, t) = \Sigma \, A_n \cos(n \, \pi \, x/L) \exp[-(n \, \pi/L)^2 \, D \, t] \, , \tag{8}$$

where the sum is over n = 0, 1, 2, … and the Fourier coefficients A_n are determined from the initial concentration $c(x, 0)$. In Appendix A we give the values of A_n for an initial concentration, $c(x, 0) = c_0 \exp[\sigma \, x]$, which is typical for steady-state electrophoresis. Following Harned and French, we consider the difference of concentrations at two different positions at the same time:

$$\Delta c \equiv c(x_2, t) - c(x_1, t) \, . \tag{9}$$

From Eq. (8) we see that all of the x-dependence in $c(x, t)$ is in the factor $\cos(n \, \pi \, x/L)$; hence, with $x_1 \equiv m_1 L$ and $x_2 \equiv m_2 L$, Δc contains the factor

$$\cos(n \, \pi \, m_2) - \cos(n \, \pi \, m_1) = -2 \sin[n \, \pi (m_1 + m_2)/2] \\ \sin[n \, \pi (m_2 - m_1)/2] \, . \tag{10}$$

Thus if $m_1 + m_2 = 1$, the first sine factor makes all n = even terms vanish in Δc. Harned and French choose $m_1 = 1/6$, $m_2 = 5/6$, which also removes the n = 3 term in the sum over

n for Δc. We generally choose $m_1 = 1/3$, $m_2 = 2/3$ because the image of the cuvette is distorted by reflections near the membranes.

In any case, as long as $m_1 + m_2 = 1$, the series for Δc is dominated for "long times", viz. $(\pi/L)^2 D t > 1$, by the $n = 1$ term:

$$\Delta c = B \exp[-(\pi/L)^2 D t] + \{\text{terms of the order } \exp[-9(\pi/L)^2 D t]\} , \quad (11)$$

where B is a constant independent of x and t, depending on the initial condition, L, m_1 and m_2 (see Appendix A).

Hence, dropping the higher order terms,

$$\ln(\Delta c) = \ln B - (\pi/L)^2 D t , \quad (12)$$

and we see that D can be determined from the slope of a plot of $-(L/\pi)^2 \ln(\Delta c)$ vs. t, as illustrated by the data from a simulation presented in Fig. 1. Errors in precisely selecting m_1 and m_2 for real data lead to a contribution from the $n = 2$ term, but it will be small compared to the dominant $n = 1$ term for large times. Data from a diffusion experiment are presented in Fig. 2. To calculate D, the pixel corresponding to the lower membrane is identified and the conjugate positions located using the known distance per pixel. The error in locating the lower membrane is less than 100 μm (5% of the total cuvette length). Calculations using the simulated experiment of Fig. 1 show that such an error in identifying the conjugate positions results in an error of ≤4% in D. The resulting plot of $-(L/\pi)^2 \ln(\Delta c)$ vs. t is linear after approximately 80 minutes (Fig. 3). A value of $D = (9.9 \pm 1.1) \times 10^{-7}$ cm^2/sec for $p(dA)_{20} \cdot p(dT)_{20}$ was obtained from the linear portion of the data.

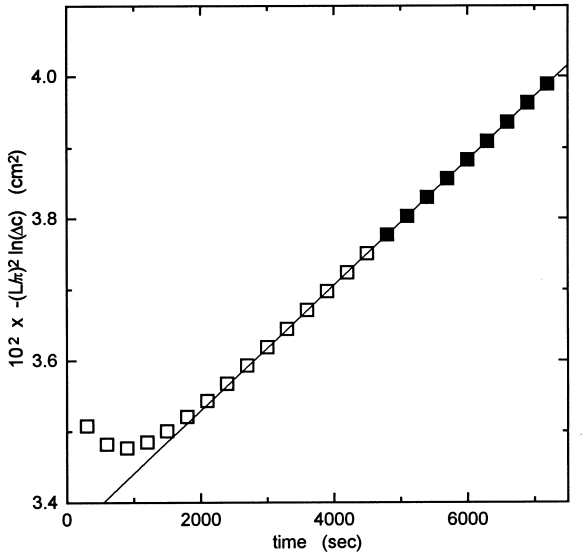

Fig. 1 Simulated data for the diffusion of a macroion. The *solid squares* satisfy the criteria $(\pi/L)^2 D t > 1$. These data were used to determine D, the regression yielding a value of $D = (8.85 \pm 0.03) \times 10^{-7}$ cm^2/s, in agreement with the set parameter of the simulation. The *open squares* do not satisfy the above criteria for linearity. The parameters of the simulation were $L = 0.2$ cm, $\Delta x = L/512$, $D = 8.85 \times 10^{-7}$ cm^2/s and $t_i = 0.05$ s. The starting condition was a steady-state exponential distribution with $\sigma = 20.01$ and $c_0 = 0.014925$ mg/ml. The 1/3, 2/3 conjugate were used in the calculation

Determining D when E≠0: When a nonzero, constant E field is present Eqs. (3) to (5) apply. It is still possible, as in the $E = 0$ case, to construct an exact Fourier series solution for $c(x, t)$ satisfying the boundary conditions. In Appendix B we give some details of the solution and show that no simple analog of the Harned and French method

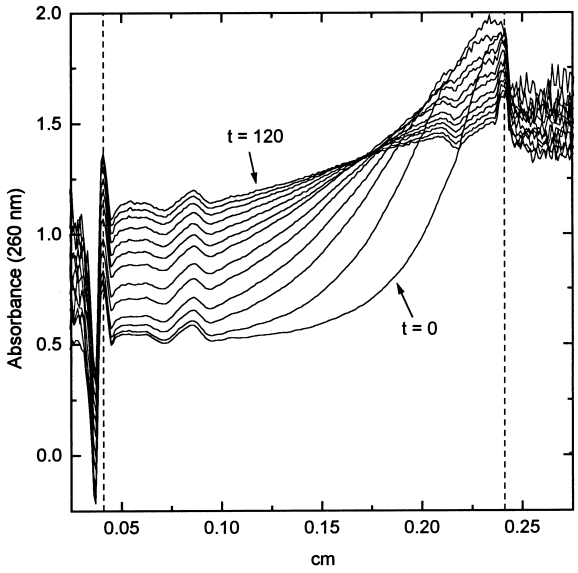

Fig. 2 Diffusion of the oligonucleotide $p(dA)_{20} \cdot p(dT)_{20}$. Absorbance profiles were taken at 10 minute intervals, commencing at $t = 0$ with a steady-state exponential gradient with $\sigma = 28.4$. The concentration of DNA in the cuvette prior to electrophoresis was 210 μg/ml. The *dashed vertical lines* mark the approximate locations of the upper (left of image) and lower membranes of the 2 mm cuvette. Distortions due to reflection (at $x < 0.1$ and $x > 0.2$) can be seen near both membranes

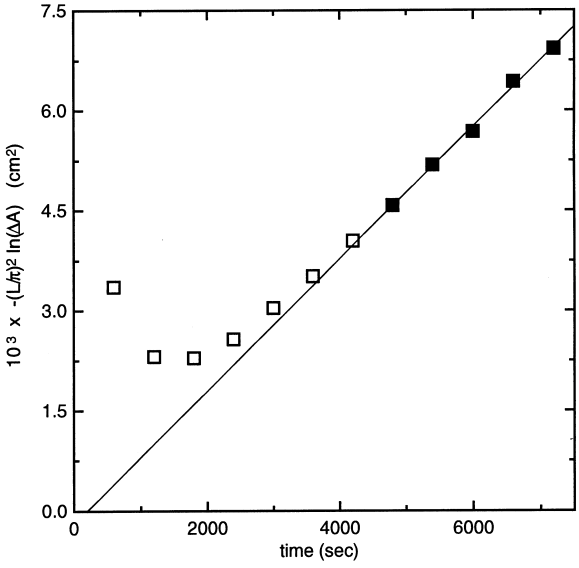

Fig. 3 Determination of D for $p(dA)_{20} \cdot p(dT)_{20}$. The 1/3, 2/3 conjugate positions were used to calculate ΔA from the data in Fig. 2. The *solid squares*, which satisfy the criteria $(\pi/L)^2 D t > 1$, were used in determining D. The slope of the line yields a value of $D = (9.9 \pm 1.1) \times 10^{-7}$ cm^2/s

exists to isolate the diffusion coefficient for the $E \neq 0$ case. If it were possible to simultaneously determine the mobility, then the steady state concentration gradient would directly give D.

Instead we show that a Fourier transform method, which essentially ignores the boundary conditions, allows us to find a solution that can be used to extract the phenomenological effective diffusion coefficient. Applying a Fourier transform (with respect to x) to Eq. (4), and treating the interval as infinite (ignoring the boundaries), it is easy to derive

$$c(x,t) = \left(1/\sqrt{4\pi D t}\right) \int_{-\infty}^{\infty} dx'\, c(x',0) \cdot \exp\left[-\{x' - (x - \mu E t)\}^2/(4 D t)\right]. \quad (13)$$

We consider an initial condition of constant concentration in the cell before the external field is turned on:

$$c(x,0) = c_0 \quad \text{for} \quad 0 \le x \le L, \quad (14)$$

and $c(x,0) = 0$ outside this range. Then Eq. (13) becomes

$$c(x,t) = \left(c_0/\sqrt{4\pi D t}\right) \int_0^L dx'\, \exp\left[-\{x' - (x - \mu E t)\}^2/(4Dt)\right] = (c_0/2)\left[\mathrm{erf}\left\{(x - \mu E t)/\sqrt{4Dt}\right\} - \mathrm{erf}\left\{(x - \mu E t - L)/\sqrt{4Dt}\right\}\right]. \quad (15)$$

It is the derivative with respect to time that we shall find to be more useful:

$$\frac{\partial c}{\partial t} = -\left[c_0/\sqrt{16\pi D}\right] t^{-3/2} \cdot \left\{\begin{array}{l}(x + \mu E t)\exp\left[-(x - \mu E t)^2/(4Dt)\right] - \\ (x + \mu E t - L)\exp\left[-(x - \mu E t - L)^2/(4Dt)\right]\end{array}\right\} \quad (16)$$

This expression for $\partial c/\partial t$ consists of a sum of Gaussian distributions (modulated by factors) with a peak that moves in time with velocity $v = \mu E$ and with a width, $w = \sqrt{4Dt}$, that spreads in time. (It is from the velocity of the peak that the mobility, μ, is determined.)

The factor $w = \sqrt{4Dt}$ in Eq. (13) is characteristic of all one-dimensional diffusion processes. In Appendix C we illustrate this with calculations for some other initial conditions.

In the region near the peak of the Gaussian where $x \approx \mu E t$, the second term in Eq. (16) can be ignored, and the simple form

$$\frac{\partial c}{\partial t} = -\left[c_0/\sqrt{16\pi D}\right] t^{-3/2} (x + \mu E t) \cdot \exp\left[-(x - \mu E t)^2/(4Dt)\right], \quad (17)$$

which neglects the boundary conditions, (Eq. (5)), is a good approximation for times long enough that the macroion boundary has mostly moved away from the upper membrane and is yet to approach the lower membrane (see below). In Appendix D we briefly indicate how an improved analytical solution incorporating the boundary conditions may be obtained.

Using real data, we must, of course, approximate $\partial c/\partial t$ by the finite difference expression $\Delta c/\Delta t$. For this approximation to be valid, during the time interval Δt the peak of the Gaussian must move a distance small compared to the

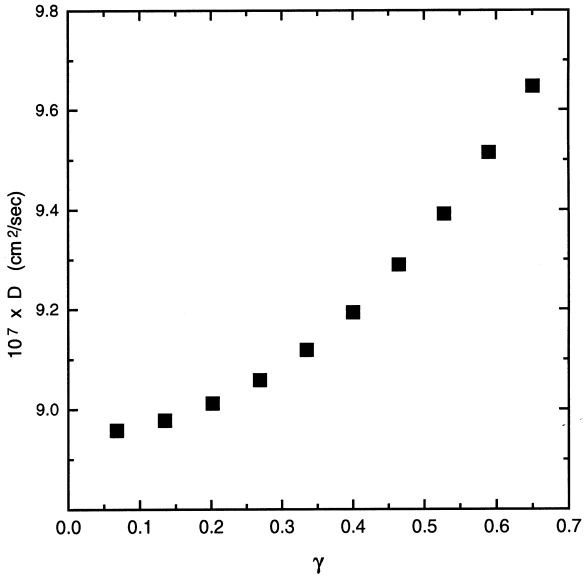

Fig. 4 The error in D introduced by the finite difference approximation. Simulated data was generated using the parameters $E = 3.0$ V/cm, $L = 0.4$ cm, $\Delta x = L/10200$, $D = 8.85 \times 10^{-7}$ cm^2/s and $t_i = 0.0005$ s, with the starting condition a uniform distribution with $c_0 = 200$ μg/ml. Data from this simulation was fitted to Eq. (17) using $\Delta c/\Delta t$ to approximate $\partial c/\partial t$. Values of D were calculated for $t = 200$ s, for the range $2 \le \Delta t \le 20$ s

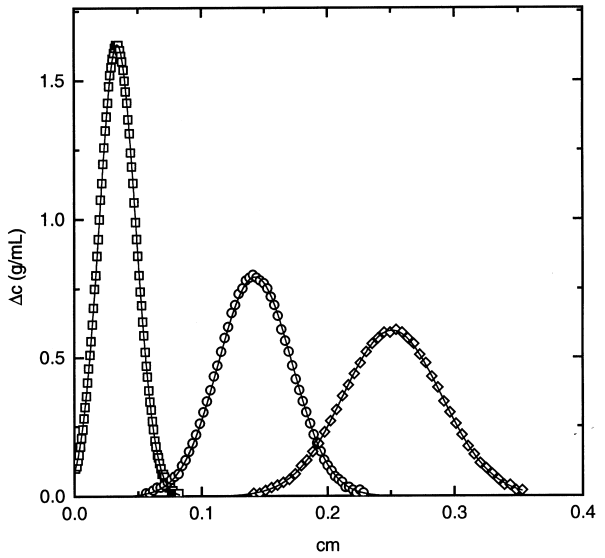

Fig. 5 Simulated electrophoresis data fitted to Eq. (20) at times; (□) 120 s, (○) 480 s, and (◇) 840 s. Not all the points used in fitting the data are displayed. The parameters of the simulation were $E = 1.0$ V/cm, $L = 0.4$ cm, $\Delta x = L/3400$, $D = 8.85 \times 10^{-7}$ cm^2/s and $t_i = 0.0015$ s. The starting condition was a uniform distribution with $c_0 = 200$ μg/ml. The time between scans used to calculate $\Delta c/\Delta t$ was $\Delta t = 0.6$ s

amount that the width has spread due to diffusion:

$$\gamma = \mu E \Delta t/\sqrt{4Dt} \ll 1. \quad (18)$$

Otherwise the motion of the peak will inadvertently be included as part of the width increase due to diffusion. The error introduced by the finite difference approximation clearly increases as E and Δt increase and as t decreases. Simulations have been used to investigate the overestimation of D as a function of γ (Fig. 4). In practice, data are readily obtained with $\gamma < 0.5$, so that the error in D is less than 5%.

When Eq. (17) is used to obtain D, restricted diffusion at the upper membrane introduces an error in D that diminishes with increasing time. Uncertainties in t, non-uniform initial conditions; e.g., due to non-flat membranes (see Appendix C and simulations below), and possible interactions between macroions and the membrane are additional sources of error in real data. We compensate for these uncertainties by defining

$$w^2 = 4Dt^* = 4Dt + \alpha \quad (19)$$

where α is a constant, and substituting w^2 for $4Dt$ in Eq. (17). Data are fitted to the equation

$$\Delta c/\Delta t = A(x + \mu E t)\exp[-(x - \mu E t)^2/w^2] \quad (20)$$

where $A = -[c_0/\sqrt{16\pi D}]\,t^{-3/2}$ (Fig. 5). A good fit to the simulated data is obtained when the macroion boundary is clear of the membranes. D is determined from the slope of a graph of $w^2/4$ vs. t (Fig. 6). The approach exactly corrects for uncertainties in t, and approximately compensates for other uncertainties (Fig. 7). In this figure the plot is concave upward, leading to an underestimate of D. However, even the extreme starting condition used in this simulation gives a value of D only 5% below the true value.

To illustrate the method we present data for electrophoresis of $p(dA)_{20}\cdot p(dT)_{20}$ at E = 1.0 V/cm, with images of the cuvette collected at $\Delta t = 20$ second intervals. Successive images are subtracted to obtain $\Delta c/\Delta t$, and fitted to Eq. (20) (Fig. 8). A value of $D = (11.9 \pm 0.7)\times 10^{-7}$ cm^2/sec for $p(dA)_{20}\cdot p(dT)_{20}$ was obtained from the slope of the $w^2/4$ vs. t graph (Fig. 9).

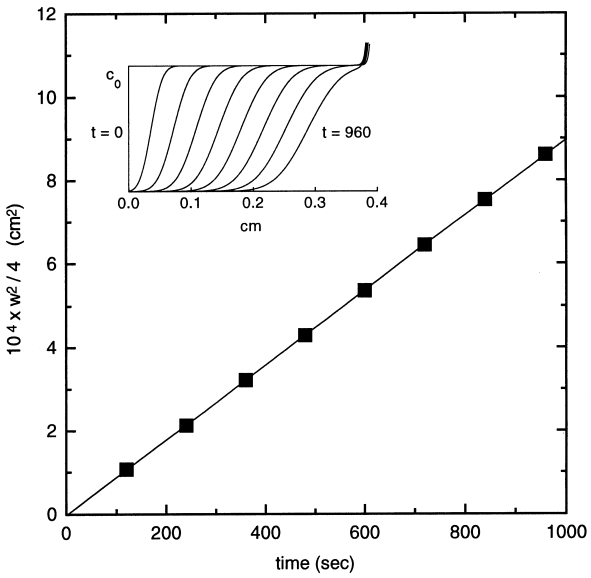

Fig. 6 Determination of the diffusion coefficient from the simulated electrophoresis data of Fig. 5. The slope of the line gives a value of $D = (8.99 \pm 0.03)\times 10^{-7}$ cm^2/s. The discrepancy between this value and the set parameter of the simulation can be attributed to the finite nature of the simulation and to approximations involved in Eq. (20). The *inset* shows the concentration distribution at 120 s intervals for comparison with Fig. 7

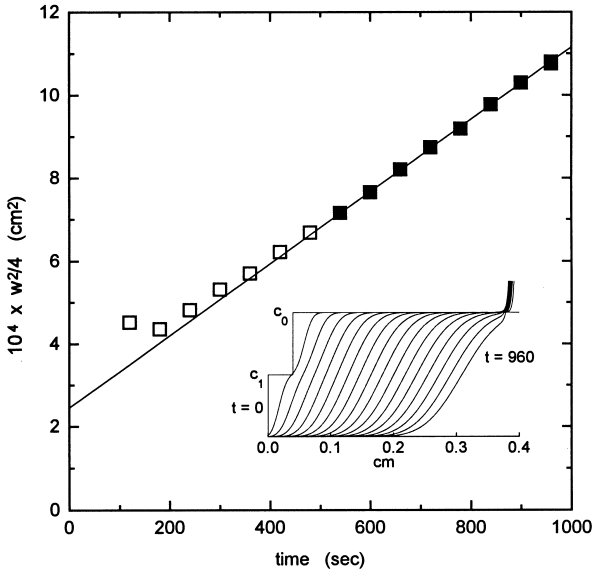

Fig. 7 The effect of non-uniform starting conditions on the determination of D. An identical simulation to that in Figs. 5 and 6 was performed, commencing with the non-uniform condition shown in the *inset*. c_1=100 μg/ml and the "step" is 0.04 cm. The slope of the line, fitted to data for $t > 500$ s, gives a value of $D = (8.4 \pm 0.2)\times 10^{-7}$ cm^2/s

Discussion

The method of Harned and French (1945) has been modified in order to measure macroion diffusion coefficients in the absence of an electric field using the AEA. It is advantageous to use the shorter 2 mm cuvettes for this method, as the time required to attain linearity in the plot of ln(Δc) vs. t increases with cuvette length.

It is not possible to exactly locate the membranes in the image of the cuvette, creating an uncertainty in the location of the conjugate positions. This error results in a contribution from the even terms in the sum for Δc, but this becomes less significant with increasing time. In practice, we find that the maximum uncertainty of 100 μm in the location of the membranes in the cuvette image produces a 4% error in the estimate of D.

It should be noted that the method does not depend on the starting conditions, and there is no requirement to know the values for the Fourier coefficients of Eq. (8) or the coefficient B in Eq. (12). However, we find it convenient to

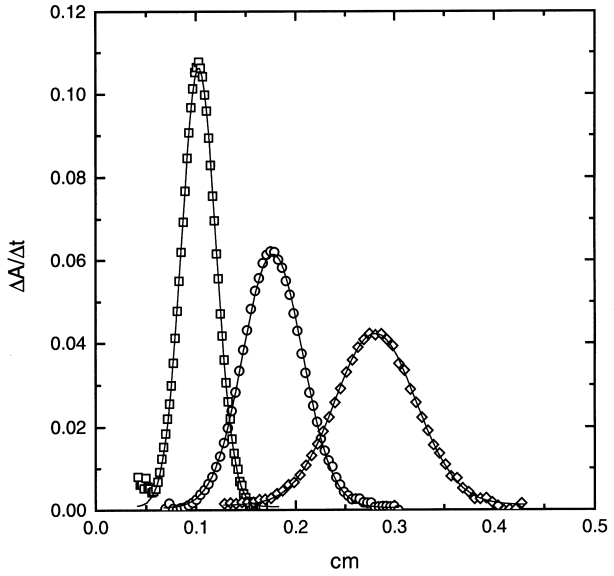

Fig. 8 Electrophoresis of 180 μg/ml $p(dA)_{20}\cdot p(dT)_{20}$ and E = 1.0 V/cm. Data for times (□) 130 s, (○) 370 s, and (◇) 710 s were fitted to Eq. (20). Not all the points used in fitting the data are displayed. The time between scans used to calculate ΔA/Δt was Δt = 20 s. The approximate locations of the upper and lower membranes is 0.04 cm and 0.44 cm, respectively

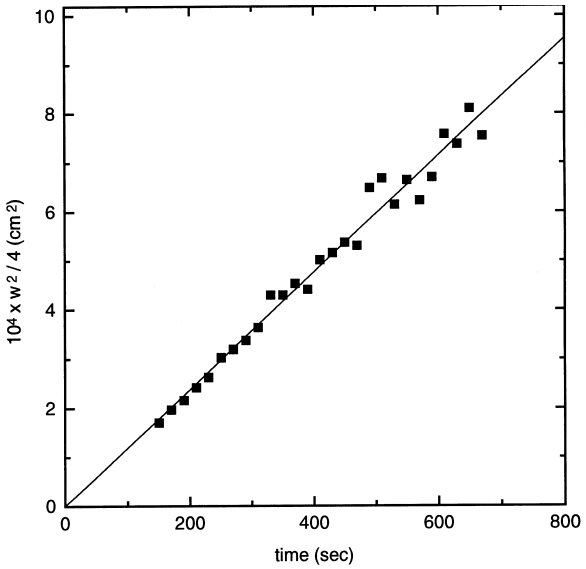

Fig. 9 Determination of the diffusion coefficient of $p(dA)_{20}\cdot p(dT)_{20}$ from the data of Fig. 8. The slope of the line gives a value of $D = (11.9 \pm 0.7) \times 10^{-7}$ cm^2/s

commence the experiment with a steady-state gradient, and the values of the above coefficients for this starting condition are given in Appendix A.

A different approach was required to determine the phenomenological diffusion coefficient of a macroion in the presence of an electric field. We use a Fourier transform method which ignores the boundary conditions and show that this approach yields a good approximation to both simulated and experimental data when the macroion boundary is clear of the membranes which seal the cuvette. (The distortion of the image close to the membranes imposes an equivalent constraint.) For these reasons it is advantageous to use the longer 4 mm cuvette in order to acquire sufficient data to generate a linear $w^2/4$ vs. t plot.

We choose to use the time derivative when analyzing real data because subtraction of successive scans removes much of the systematic noise present in the image of the cuvette. Analysis of single images using Eq. (15) is possible but the greater noise in the data results in greater uncertainty in D.

For the initial condition given by Eq. (14), a plot of $w^2/4$ vs. t is expected to have a positive intercept with the abscissa due to restricted diffusion at the upper membrane. This is seen in the simulation presented in Fig. 6. With irregular starting conditions, as in Fig. 7, this intercept shifts to the left. The negative intercept of the abscissa seen in the experimental data (Fig. 9) is consistent with the presence of imperfections in the shape of the upper membrane.

The requirement that the macroion boundary be free of the membranes limits the range of electric fields at which measurements can be made. It is not possible to determine D (or μ) at the low electric fields used in steady-state experiments because macroions never clear the upper membrane. The exact solution to the $E \neq 0$ case presented in Appendix B could form the basis of a solution to this problem and is currently under investigation.

In summary, we have demonstrated the feasibility of using approximate analytic solutions to the differential equations and boundary conditions describing diffusion in the AEA to determine effective macroion diffusion coefficients. The solutions are good approximations to numerical simulations of the differential equations, and provide a good phenomenological description of the experimental data for the oligonucleotide $p(dA)_{20}\cdot p(dT)_{20}$ in 100 mM KCl, 20 mM Tris-Cl, pH 8.0. Diffusion measurements are made on the sample used for electrophoresis, at the same macroion concentration, in the same buffer, so that data are directly comparable. Values of D obtained by the above methods will assist in the interpretation of electrophoresis experiments conducted as part of our research into the charge and hydrodynamic properties of macroions.

Acknowledgements We thank Jan Heirtzler and Ian MacGregor for excellent technical assistance. This work was funded by NSF grant BIR-9314040 to TML. HKS gratefully acknowledges partial supported received from the Office of the Vice President for Research of the University of New Hampshire.

Appendix A: Some details of the E = 0 series solution

The values of the Fourier coefficients, A_n, in Eq. (8) for an initial concentration, $c(x, 0) = c_0 \exp[\sigma x]$ follow directly from the orthogonality of the $\cos(n\pi x/L)$ functions. We find

$$A_0 = (c_0/L\sigma)\,(e^{L\sigma}-1)$$

$$A_n = (2c_0\sigma/L)\,((-1)^n e^{L\sigma}-1)/(\sigma^2+(n\pi/L)^2).$$

The coefficient B in the n = 1 term in Δc, Eq. (11), follows from A_1.

We find

$$B = [(4c_0\sigma/L)\,(e^{L\sigma}+1)/(\sigma^2+(\pi/L)^2)]\,\sin[(m_2-m_1)\,\pi/2].$$

Appendix B: Some details of the E≠0 Fourier series solution

The boundary value problem described by Eqs. (3) to (5) can be solved by a straightforward separation of variables technique. One finds

$$c(x,t) = c_E \exp[\mu E x/D] + \exp[\mu E x/2D]\exp[-(\mu E)^2 t/4D] \cdot \sum_{n=0}^{\infty} A_n \exp[-(n\pi/L)^2 D t][\cos(n\pi x/L) + (\mu E L/2n\pi D)\sin(n\pi x/L)],$$

where the leading term is the steady-state solution, (when c becomes independent of time, $\partial c/\partial t = 0$), and the coefficients c_E and A_n are determined by the initial conditions. Obviously the steady-state concentration gradient gives D directly if μ and E are known.

If we proceed as in the E = 0 case and try to use the Harned and French method expanding for large t, ($(\pi/L)^2 D t > 1$), keeping only the n = 0 and n = 1 terms, we find

$$c(x,t) \to c_E \exp[\mu E x/D] + \exp[\mu E x/2D]\exp[-(\mu E)^2 t/4D] \cdot \{A_0(1+\mu E x/2D) + A_1 \exp[-(\pi/L)^2 D t] \cdot [\cos(\pi x/L) + (\mu E L/2\pi D)\sin(\pi x/L)]\}.$$

If we now form a concentration difference at two different x-values, the leading term varies with x and does not cancel out as in the E = 0 case. In fact the solution is dominated by the steady-state term which is approached rapidly for large times if E is not too small.

Appendix C: Effect of non-uniform initial condition

As examples, we present two simple analytical calculations of c(x, t) for non-uniform initial conditions. If instead of the uniform initial condition given by Eq. (14), we assume

$$c(x, 0) = c_0\,(1 - e^{-ax}),$$

then instead of Eq. (15), we find

$$c(x,t) = (c_0/2)\,\mathrm{erf}\left[(x-\mu E t)/\sqrt{4Dt}\right] - (c_0/2)\exp[-a(x-\mu E t + a D t)] \cdot \mathrm{erf}\left[(x-\mu E t - 2a D t)/\sqrt{4Dt}\right].$$

With the initial condition

$$c(x, 0) = c_1 \text{ for } 0 \le x \le x_0 \text{ and } c(x, 0) = c_0 \text{ for } x_0 \le x \le L,$$

we find

$$c(x,t) = (c_1/2)\,\mathrm{erf}\left[(x-\mu E t)/\sqrt{4Dt}\right] + [(c_0-c_1)/2]\,\mathrm{erf}\left[(x-x_0-\mu E t)/\sqrt{4Dt}\right] - (c_0/2)\,\mathrm{erf}\left[(x-\mu E t - L)/\sqrt{4Dt}\right].$$

This starting condition is used in the simulation presented in Fig. 7, with $x_0 = L/10$ and $c_1 = c_0/2$.

Appendix D: Improving the analytic solution for E≠0

To include the boundary condition, Eq. (5), in the solution of the diffusion equation, Eq. (4), several approaches are possible. One is to make a Laplace transform in t. The boundary conditions at the membranes can then be imposed rather easily; the difficulty arises in computing the inverse Laplace transform. Here an expansion for short times or a saddle point approximation are possible approaches. The resulting expansions are complicated and do not seem necessary for the work presented in this paper.

Another approach based on a useful change of dependent variable introduced by Furth,

$$c^* = c \exp[-(v/2D)\,(x - x_0) + v^2 t/4D],$$

where $v = \mu E$, is described in the book by Jost (1952).

References

Booth F (1950) Cataphoresis of spherical, solid non-conducting particles in a symmetrical electrolyte. Proc R Soc A 203:514–533

Cox D (1965) Computer simulation of sedimentation in the ultracentrifuge. I. Diffusion. Arch Biochem Biophys 112:249–258

Cox D, Dale R (1981) Simulation of transport experiments for interacting systems. In: Frieden C, Nichol L (eds) Protein-protein interactions. Wiley, New York, pp 173–211

Gosting L (1956) Measurement and interpretation of diffusion coefficients of proteins. Adv Protein Chem 11:429–554

Harned H, French D (1945) A conductance method for the determination of the diffusion coefficients of electrolytes. Ann New York Acad Sci 46:267–281

Henry D (1931) The cataphoresis of suspended particles. Part I. The equation of cataphoresis. Proc Royal Soc London Ser A 133:106–129

Jost W (1952) Diffusion in solids, liquids, gases. Academic Press, New York, pp 47–50

Laue T, Hazard A, Ridgeway T, Yphantis D (1989) Direct determination of macromolecular charge by equilibrium electrophoresis. Anal Biochem 182:377–382

Laue T, Ridgeway T, Wooll J, Shepard H, Moody T, Wilson T, Chaires J, Stevenson D (1996) Insights from a new analytical electrophoresis apparatus. J Pharm Sci 85:1331–1335

Onsager L, Fuoss R (1932) Irreversible processes in electrolytes. Diffusion, conductance, and viscous flow in arbitrary mixtures of strong electrolytes. J Phys Chem 36:2689–2778

Onsager L (1945) Theories and problems of liquid diffusion. Ann New York Acad Sci 46:241–265

Overbeek J, Wiersema P (1967) The interpretation of electrophoretic mobilities. In: Bier M (ed) Electrophoresis: theory, applications + technique, vol II. Acad Press, New York, pp 1–52

Ridgeway T, Hayes D, Anderson A, Levasseur J, Demaine P, Kenty B, Laue T (1994) Possible clinical applications for direct molecular charge determination by equilibrium electrophoresis. SPIE Proceedings 2136:263–274